The Journal of Experimental Biology 209, 3742-3757
Published by The Company of Biologists 2006
doi:10.1242/jeb.02439

Centre of mass movement and mechanical energy fluctuation during gallop locomotion in the Thoroughbred racehorse

Thilo Pfau[1,*], Thomas H. Witte[1,†] and Alan M. Wilson[1,2]

[1]*Structure and Motion Laboratory, The Royal Veterinary College, University of London, Hawkshead Lane, North Mymms, Hatfield, AL9 7TA, UK and* [2]*Structure and Motion Laboratory, University College London, Royal National Orthopaedic Hospital, Brockley Hill, Stanmore, Middlesex, HA7 4LP, UK*

*Author for correspondence (e-mail: tpfau@rvc.ac.uk)

†Present address: Cornell University Hospital for Animals, Box 25, Ithaca, NY 14853, USA

Accepted 11 July 2006

Summary

During locomotion cyclical interchange between different forms of mechanical energy enhances economy; however, 100% efficiency cannot be achieved and ultimately some mechanical work must be performed *de novo*. There is a metabolic cost associated with fluctuations in mechanical energy, even in the most efficient animals. In this study we investigate the exchanges between different forms of mechanical energy involved in high-speed gallop locomotion in Thoroughbred race horses during over-ground locomotion using innovative, mobile data collection techniques. We use hoof-mounted accelerometers to capture foot contact times, a GPS data logger to monitor speed and an inertial sensor mounted over the dorsal spinous processes of the fourth to sixth thoracic vertebrae (the withers) of the horse to capture trunk movement with six degrees of freedom. Trunk movement data were used to estimate the movement of the centre of mass (CoM). Linear (craniocaudal, mediolateral and dorsoventral) and rotational (roll, pitch and heading) kinematic parameters (displacement, velocity and acceleration) were calculated for seven horses at gallop speeds ranging from 7 to 17 m s^{-1} during their regular training sessions. These were used to estimate external mechanical energy (potential energy and linear kinetic energy of the CoM) as well as selected components of internal energy (angular kinetic energy). Elastic energy storage in the limbs was estimated from duty factor, sine wave assumptions and published leg stiffness values.

External mechanical energy changes were dominated by changes in craniocaudal velocity. Potential energy change, which was in phase with craniocaudal energy during the front limb stances, was small. Elastic energy storage in the limbs was small compared to the overall amplitude of fluctuation of external mechanical energy. Galloping at high speeds does not therefore fit classical spring mass mechanics.

Key words: centre of mass movement, mechanical energy, high speed locomotion, horse, biomechanics.

Introduction

Mechanical energy changes in biological systems cost energy. The spring-like properties of the limbs of animals help to moderate this cost during running through the storage and release of elastic energy; however, these mechanisms are not 100% efficient. Energy is lost from the system because tendon springs only return 90–95% of the energy originally stored in them (Ker, 1981; Riemersma and Schamhardt, 1985; Bennett et al., 1986) and because there may not be total interchange between potential, kinetic and elastic strain energy. Also, energy lost to the environment through aerodynamic drag, ground deformation etc may only be replaced during stance periods and primarily by the hind legs, due to the large proportion of muscle mass found there (Payne et al., 2004; Payne et al., 2005). Even when the average speed does not change between strides, some mechanical work must be performed *de novo* and therefore there is a metabolic cost associated with fluctuations in mechanical energy, even in the most efficient animals.

The centre of mass (CoM) of an animal is the point inside or outside the body at which the entire mass of the subject can be considered to be concentrated. External work of locomotion is defined as the work required to transport the CoM, and in limbed animals this is achieved by cyclical movement of the limbs. The total external mechanical energy associated with this type of locomotion is equal to the sum of the kinetic and potential energies of the CoM. Although few biological analogies exist, the optimum method of transporting a mass over ground is the wheel, being able to maintain constant forward velocity and constant vertical position, and thereby

minimising costly conversions of energy from one form to another in biological systems (Minetti, 2000). Recently, it has been shown that when humans travel without CoM oscillations they do so at a higher cost than by not doing so (Ortega and Farley, 2005). However, it is likely that biology has attempted to optimise locomotion to be energetically efficient. In particular, cursorial animals, which must travel long distances at the minimum energetic cost, are likely to have evolved mechanisms by which fluctuations in mechanical energy can be avoided or minimised.

Conventionally, gaits are categorised as walking or running depending upon the phase relationships of the fluctuations in kinetic and potential energies during the stride cycle (Cavagna et al., 1977; Ahn et al., 2004). Walking gaits classically demonstrate an out-of-phase relationship between these two energy forms, with pendulum-like exchange helping to maintain a relatively constant total mechanical energy. In contrast, during running, the fluctuations of kinetic and potential energies are in phase and elastic energy storage helps to compensate for the decrease in mechanical energy during the stance phases, much like a bouncing ball or a pogo stick. Galloping at low to medium speeds, however, fits neither the inverted pendulum nor the bouncing ball paradigms well, with a combination of spring-like and vaulting mechanisms described for horses (Minetti et al., 1999) and dogs (Cavagna et al., 1977). Galloping in horses has therefore been likened to bipedal skipping (Minetti, 1998). Measurements of skipping and galloping have shown that a combination of both elastic and inverted pendulum energy-saving mechanisms may be at work in these gaits. It remains likely, however, that a novel mechanistic description based on collision events is required (Ruina et al., 2005). Mechanical energy also exists as internal work or the movements of body segments relative to the CoM and rotation of the body around the CoM. In the horse the limbs represent a small portion of the total mass and the large trunk has significant angular inertia. A large part of the internal work will therefore consist of changes in rotational energies of the trunk around the CoM.

Measurements of the mechanical energy of animals have traditionally been made using kinematics studies. However, for higher speed gaits treadmills are necessary to allow the collection of repeated strides at a controlled speed. Large marker sets are required to describe the three-dimensional motion of all body segments (Buchner et al., 2000; Minetti et al., 1999). Motion data, together with inertial data for each body segment, are subsequently used to compute displacements of the CoM and internal work (Buchner et al., 1997). Treadmill locomotion, however, creates artefacts in the gait patterns of animals, which lead to increased vertical trunk oscillations (Buchner et al., 1994; Barrey et al., 1993). This is particularly important when considering the mechanical energy of the animal. In addition, energy transfer between the treadmill and the subject may be an important confounding factor (Savelberg et al., 1998) and treadmills offer only a limited range of speeds (typically up to 15 m s^{-1} for horses) for the study of high quality animals. Measurements of the trajectory of the CoM during very fast exercise have therefore not been performed. The maximum speed at which such measurements have been made is 12 m s^{-1} (Minetti et al., 1999).

A good estimate of CoM displacement can be gained from the measurement of the overall trunk movement (Buchner et al., 2000). This is especially true for large cursorial animals because they have relatively low limb masses (e.g. 5.8% and 5.5% of the total body mass for the hind limbs and fore limbs of the horse, respectively) and most of the limb mass is proximal. Although visceral movements will cause the CoM to change location within the trunk, this factor can only be quantified by the use of force platforms as ergometers (Cavagna, 1975). Models have been developed which attempt to quantify visceral displacements; however, these rely on detailed cinematographic and dynamometric measurements as well as knowledge of the visceral mass (Minetti and Belli, 1994). Recently, a six degree-of-freedom (d.f.) inertial sensor has been shown to provide accurate trunk movement data for horses during treadmill locomotion by integration from 3D accelerations assuming cyclical movement over a series of strides (Pfau et al., 2005). Angular velocities from the sensor along with estimates of whole body inertia can be used to estimate internal work related to trunk movement.

Equine gallop is a poorly understood gait and difficult to study, particularly at the highest speeds. The goal of the present study was to test the hypothesis that the energetics of gallop locomotion under field conditions at truly high speeds fit neither the inverted pendulum nor the spring mass paradigms of terrestrial locomotion. We estimate body mechanical energy changes during high speed gallop exercise under field conditions from an inertial sensor attached to the trunk of a horse. The speed dependence of translational and rotational trunk displacements, velocities and accelerations were documented. From these data, CoM displacement and the associated mechanical energy were estimated.

Materials and methods

Data collection

Seven clinically sound Thoroughbred racehorses of mean age 2.9 years (range 2–5 years) and mean mass 480 kg (range 460–500 kg) were used in this study. The animals were stabled at a single yard and were all undergoing the same regime of flat race training. Prior to testing the mass of each horse was measured using standard equine weighing scales. The mass of the jockey and riding equipment was 63.5 kg.

Each horse was equipped with a modified 6 d.f. inertial sensor (MT9, Xsens Technologies, B.V., Enschede, The Netherlands) and four foot-mounted accelerometers (ADXL150, sensitivity 38 mV g^{-1}, Analog devices; Norwood, MA, US), and the jockey with a GPS data logger (modified G30-L, Laipac Technology Inc., Ontario, Canada). The inertial sensor comprises a three-axial accelerometer (max. 10 g) a three-axial gyroscope (max. 900 degrees s^{-1}), three magnetometers and a thermometer. Inertial sensor data were low-pass filtered (analog low-pass filter, 50 Hz cut-off

frequency for accelerometers and gyroscopes, 10 Hz for magnetometers) and subsequently AD converted. The sensor was mounted in a custom-made harness constructed of malleable casting material (Dynacast, Smith and Nephews, Wound Management, Hull, UK) over the spinous processes of the fourth–sixth thoracic vertebrae (the withers) of the horse, beneath the forwardmost edge of the saddle. A cable ran from the sensor, between the saddle pads under the saddle, to a DECT (Digital Enhanced Cordless Telecommunications) telemetry unit (HW8612, Höft & Wessel, Hannover, Germany) and battery pack mounted on a waistband worn by the jockey. A cable ran from the telemetry unit to an antenna, which was mounted on the jockey's skullcap. Serial data from the sensor (at 115 200 bit s^{-1}) were transmitted at 1.88–1.90 GHz using DECT-CLDPS (ConnectionLess Data Packet Service), an extension of the DECT telephone standard tailored for general data transmission, which handles up to six data streams of a combined bandwidth of 460 kbit s^{-1}. The mobile DECT telemetry receiver and laptop computer were mounted in a vehicle, which stayed within range of the exercising horses. Data were recorded at 250 samples individual $sensor^{-1}$ s^{-1} *via* custom software written in Microsoft Visual C++ (Microsoft Corp., Redmond, WA, USA) using the sensor's software development kit (SDK, Xsens). Data files consisted of ten channels; the calibrated output from three accelerometers, three gyroscopes, three magnetometers and the sensor temperature, each at 250 samples s^{-1}.

A stand-alone Global Positioning System (GPS) device (modified G30-L, Laipac Technology Inc., Ontario, Canada) was configured to log the GPRMC GPS data once per second (Witte and Wilson, 2004; Witte and Wilson, 2005). GPRMC data consist of speed (knots), position (latitude and longitude), time (Universal Time Constant) and date. The GPS device (dimensions 70 mm×50 mm×25 mm and mass 95 g) was mounted securely on the rider's hat by means of a custom-made elastic strap and was powered on as the horses left the yard. Data were logged continuously from this time until the horses returned from exercise.

Foot-on and foot-off events of all four limbs were determined by measuring foot acceleration using solid-state capacitive accelerometers with a dynamic range of ±50 g (ADXL150, Analog devices; sensitivity 38 mV g^{-1}). These were protected by enclosure in epoxy-impregnated Kevlar fibres (total mass 2 g) and mounted at the dorsal midline of each hoof with the sensitive axis orientated in a proximo-distal direction using hot melt glue. Output signals were telemetered *via* four narrow-band analogue FM radio telemetry devices operating in the 458 MHz band range with an audio response of 9 Hz to 3 kHz at –3 dB (ST/SR500, and Douglas Ltd, Baughurst, Hampshire, UK). Data were logged at a sample rate of 1000 samples s^{-1} *via* a 12-bit A/D converter into a PCMCIA card (DAQcard700, National Instruments, Austin, TX, USA) onto a vehicle-mounted laptop computer running custom software in MATLAB (The Mathworks, Natick, MA, USA). Each telemetry transmitter and its battery were mounted within a standard elastic exercise bandage on the lateral aspect of the third metacarpal/metatarsal bone of each limb (mass of telemetry unit and battery 140 g, total mass of bandage plus telemetry unit, 310 g). A short cable running along the lateral aspect of the digit linked the telemetry unit to the accelerometer. See elsewhere for more detail (Witte et al., 2004).

The horses were ridden by their regular exercise rider during the study. They were exercised in groups of three, although data were collected from only one horse at a time. The horses were warmed up by walking and trotting for approximately 10 min on a level racetrack (Polytrack, Martin Collins, Hungerford, Berkshire, UK) and were subsequently galloped at a steady speed for 600 m before gradually accelerating to maximum speed over a further 400 m (about 80 strides). Inertial sensor, accelerometer and GPS data were collected continuously throughout the period of gallop exercise. The entire collection period lasted approximately 2 min and encompassed the entire range of exercise speeds.

Data analysis

GPS data were downloaded from the data logger using GPS Wedge Software (CommLinx Solutions Pty Ltd, Lutana, TAS, Australia). Speed and time data were extracted for each position fix using custom software written in MATLAB.

Voice transcription software 'Transcriber' (Barras et al., 1998) was used to manually identify the times of foot-on and foot-off from the accelerometer signal. Stride start times were defined from the foot on events identified in the left fore foot accelerometer signals. Foot-on and foot-off timings were used for three different purposes:

(1) Synchronisation with GPS data to obtain speed for each stride;

(2) Determination of duty factor to estimate limb force and hence elastic energy storage in the limbs through stance;

(3) Determination of stride times for integration of inertial sensor acceleration to velocity and displacement.

First, the time of the midpoint of each stride was determined and GPS speed values were interpolated to give the average speed for the stride.

Second, peak vertical ground reaction force (F_{max}) was predicted for each limb (according to Alexander et al., 1979), using a front/hind mass distribution of 57/43% (Witte et al., 2004). For each stride the lead and non-lead legs were identified from the relative timing of footfalls. Using a front limb stiffness k_f of 55 kNm^{-1} and a hind limb stiffness k_h of 40 kNm^{-1} [data from McGuigan and Wilson (McGuigan and Wilson, 2003) and hind leg stiffness by scaling using front hind impulse distribution], and assuming a sinusoidal resultant leg force–time relationship during stance (Witte et al., 2004), limb elastic energy storage was calculated at each time point during the stance phase using $E_{el}=1/2F^2/k$ (F, limb force and $k=k_f$ or $k=k_h$, respectively), similar to what has been done before (Robilliard and Wilson, 2006).

Third, initial analysis of trunk movement from the inertial sensor data followed the process described earlier (Pfau et al., 2005). Briefly, the orientation of the sensor in the form of Euler

angles representing rotations from the sensor into the global coordinate system were computed from the raw data using the sensor fusion algorithm of the MT9 software development kit (MT9 SDK, Xsens Technologies, B.V., Enschede, The Netherlands). Linear accelerations were projected from the sensor coordinate system into a horse-referenced coordinate system based on rotation matrix data. Accelerations were then double integrated to displacements based on stride segmentations gained from the signals of the hoof-mounted accelerometer on the left fore limb. Angular velocities and accelerations were derived from orientation data using numerical differentiation of a regression line fitted to 11 data points (current + 5 left and 5 right neighbouring data points).

As described above, preliminary segmentation of inertial data was performed using stride timings from the hoof-mounted accelerometer of the left fore limb. However, although the stride durations derived from the accelerometer were accurate the accelerometer could not be absolutely synchronised with the inertial sensor due to channel-dependent delays in the DECT telemetry. Therefore a trunk movement feature was used to re-segment the inertial sensor data for each individual stride. The minimum vertical velocity was chosen as a consistent feature and this feature was identified within each stride. The subsequent re-segmentation ensured that data of different horses were cut in a similar manner, although this method causes a variation of up to 4% of stride time at medium speeds. Aerial times were estimated from plotting the sum of dorsoventral kinetic and potential energy (Fig. 1) and locating the aerial phase within that area of the curve where it is approximately constant. This procedure is based on the assumption that the sum of dorsoventral kinetic energy and potential energy is constant during the aerial phase (when no feet are on the ground to produce an external ground reaction force) and the validity of this approach was confirmed through simultaneous collection of inertial sensor data and high speed video in a treadmill experiment with a cantering Thoroughbred horse. Indeed, the sum of dorsoventral kinetic energy and potential energy was found to be more constant during the aerial phase after the displacements were projected to the CoM (see next paragraph).

Based upon previous studies of inertial properties of Dutch Warmblood horses, the position of the inertial sensor was known to be some distance above and forward of the actual CoM of the horse (Fig. 2). The average position of the CoM in those horses has been shown to be 0.22 m below the withers (the location of our sensor) and about halfway between the withers and the dorsal spinous process of the fourteenth thoracic vertebra (Buchner et al., 1997). It was therefore inevitable that displacement data derived at the location of the sensor were not an accurate representation of displacements of the CoM itself. In general, rotations around the CoM result in a combination of rotation and linear displacement at any point distant from the CoM. For example, changes in the pitch orientation of the trunk would result in additional craniocaudal and dorsoventral displacements at the location of the sensor. Here, a fixed point estimate of the CoM relative to the sensor position was used. An empirical method was used to analyse the influence of the assumed position of the CoM on the

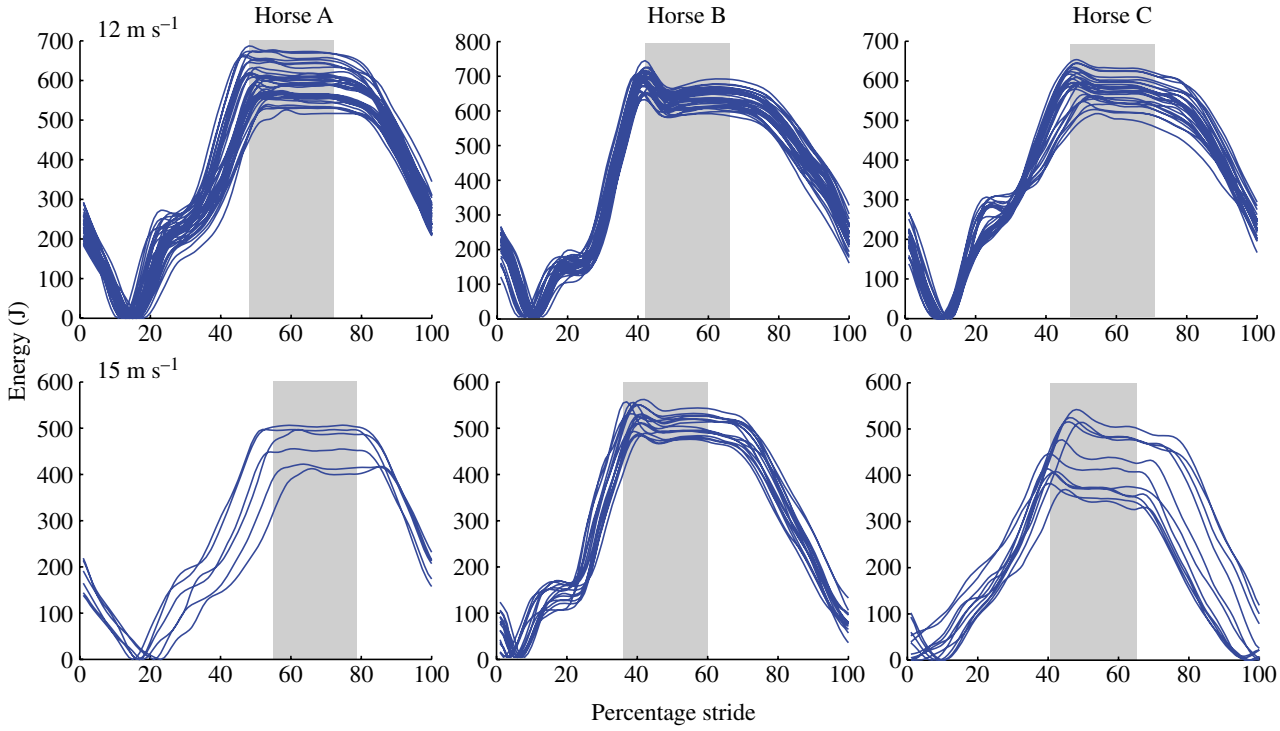

Fig. 1. Sum of potential and dorsoventral kinetic energy for the speed categories 12 m s^{-1} (11.5–12.5 m s^{-1}; top plots) and 15 m s^{-1} (14.5–15.5 m s^{-1}; bottom plots). Horses A–C are the three typical horses used in Figs 4–7, 10 and 11.

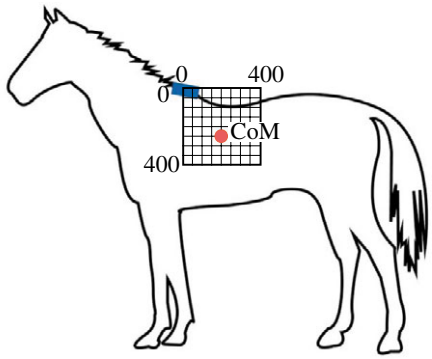

Fig. 2. Positions used for the sensitivity analysis for the relative position of the centre of mass (CoM) of a standing horse relative to the position of the inertial sensor. The sensor (blue) was mounted over the dorsal spinous processes of the fourth to sixth thoracic vertebrae (withers). The red circle shows the estimate used in this study. Values indicate mm from the sensor.

estimated external work. The amount of external mechanical work (positive changes in the sum of potential energy and the three (craniocaudal, mediolateral and dorsoventral) linear kinetic energies) was calculated over a grid of positions starting from the position of the sensor and going 400 mm backwards and downwards (in steps of 50 mm). At each of these 81 (9×9) positions the external mechanical work was calculated assuming that all measured rotations originate from a rotation around the CoM and that the relative position of the CoM does not change during the stride. The final estimate of the CoM movement was then derived from the combination of sensor linear movement and sensor orientation to calculate the movement of a fixed point estimate 250 mm below and 200 mm behind the sensor position (see Results). As discussed below (see Discussion), sensor roll was ignored at this stage of the analysis. Subsequently velocity and acceleration were calculated by numerical differentiation. Here a local regression line was fitted around each data point (of displacement, respectively, velocity data) and the slope of this line used as the velocity (respectively, acceleration) value.

Potential energy (E_p) and linear kinetic energies (E_{kx}, E_{ky}, E_{kz}) were calculated routinely ($E_p=mg\Delta h$ and $E_k=mv^2/2$, where m=mass of horse, Δh=vertical position from a datum and v=velocity), with front–back velocities constituting of the sum of the average speed for the stride (determined from the GPS data) and the mean-subtracted velocity output of the inertial sensor. In order to calculate rotational kinetic energies and hence derive an estimate of the internal work associated with trunk movement around the CoM, it was necessary to calculate the rotational moment of inertia of the animal. In the absence of detailed morphological measurements, the inertial properties of the horse were estimated by modelling the trunk as a cylinder of radius 0.3 m and length 2.0 m. This gives a volume of 0.57 m^3, which is sensible for the mass and density of a horse. Each horse's individual mass was then used to calculate roll, pitch and heading moments of inertia (I). It was then possible to calculate the kinetic energy of roll, pitch and heading ($E_k=I\omega^2/2$). The external mechanical energy of the trunk was calculated as the sum of all the linear kinetic energies and the potential energy through time. External mechanical work for each stride was calculated by summing up positive increments in total external energy over the complete stride.

Strides were categorised into 1 m s^{-1} speed categories with the speed label representing the middle value, and individual strides were interpolated to 100 samples for each variable [linear (craniocaudal, mediolateral, dorsoventral) displacements, velocities, accelerations and energies; rotational (roll, pitch, heading) displacements, velocities, accelerations and energies; and potential energy].

For each stride the maximum, minimum and range were determined for each variable of interest. Mean data were derived for each horse at each speed and a population mean calculated. The ranges and maxima were regressed against speed, median and interquartile ranges calculated, and quadratic curves were fitted to the data. Median and interquartile ranges were chosen for the maxima in order to account for the apparent non-Gaussian distributions. Quadratic curves were chosen as they consistently gave high r values, indicating they represent the general trend in the data with speed.

Results

A total of 1601 strides were collected, of which 1107 were analysed (ranges 133–210 per horse and 28–182 per speed category) during this study. The large amount of data made it necessary to use automatic computer-based procedures to divide the data into strides (see data analysis). This resulted in the exclusion of 494 strides, which could not be processed automatically, from the analysis.

The results of the sensitivity analysis to determine the influence of the assumed relative position of the CoM by calculating external mechanical work of locomotion are shown in Fig. 3. The figure shows the average mechanical work per stride for a typical horse in this study for all the locations included in the grid search. A distinct minimum can be observed in the vertical direction at 250 mm below the sensor position. The craniocaudal distance is less influential, resulting in a broad minimum around a distance of 200 mm towards the back of the horse. The following results presented in this study are based on this estimate of the position of the CoM.

Figs 4 and 5 show craniocaudal, mediolateral and dorsoventral displacement, velocity and acceleration for the speed categories 12 m s^{-1} and 15 m s^{-1}, respectively. Data from three typical horses (horses A–C) are shown. Horses were chosen based on the number of strides available for the speed categories 12 (11.5–12.5 m s^{-1}) and 15 (14.5–15.5 m s^{-1}).

Craniocaudal and dorsoventral displacement curves show sinusoidal behaviour with one clear maximum and one clear minimum per stride. Mediolateral displacement was less sinusoidal and more variable between horses. In addition, mediolateral data for horse C (Fig. 3) and horses B and C (Fig. 4) show two distinct clusters of curves constituting left

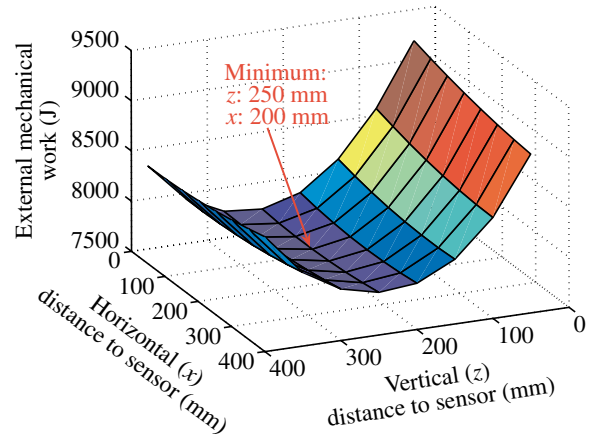

Fig. 3. Average external mechanical work per stride for different estimates of the position of the CoM relative to the position of the sensor on the horse. External mechanical work is calculated as the sum over all positive energy changes in total mechanical energy (sum of potential, and all linear kinetic energies).

and right lead gallop, respectively. Velocity curves reveal one bimodal minimum and one bimodal maximum per stride for craniocaudal velocity, and one bimodal maximum and one unimodal minimum for dorsoventral velocity. Mediolateral velocity is more variable and shows distinct curves for left and right lead gallop. Craniocaudal accelerations show a minimum at around 30% of stride duration followed by an area of near zero acceleration, which coincides approximately with a dorsoventral acceleration of around –10 m s^{-2} (1 g). Mediolateral accelerations are variable and in general small during the estimated aerial phase.

Angular parameters (12 m s^{-1}: Fig. 6, 15 m s^{-1}: Fig. 7) show consistent characteristics with pitch being most similar between horses. Pitch displacement curves show one unimodal minimum and a characteristic, broad bimodal maximum (approximately 40–60% stride time), which corresponds to a near zero pitch velocity and acceleration. During this time (aerial phase), roll and heading velocity and also acceleration appear to be small. However, this was not true for all horses.

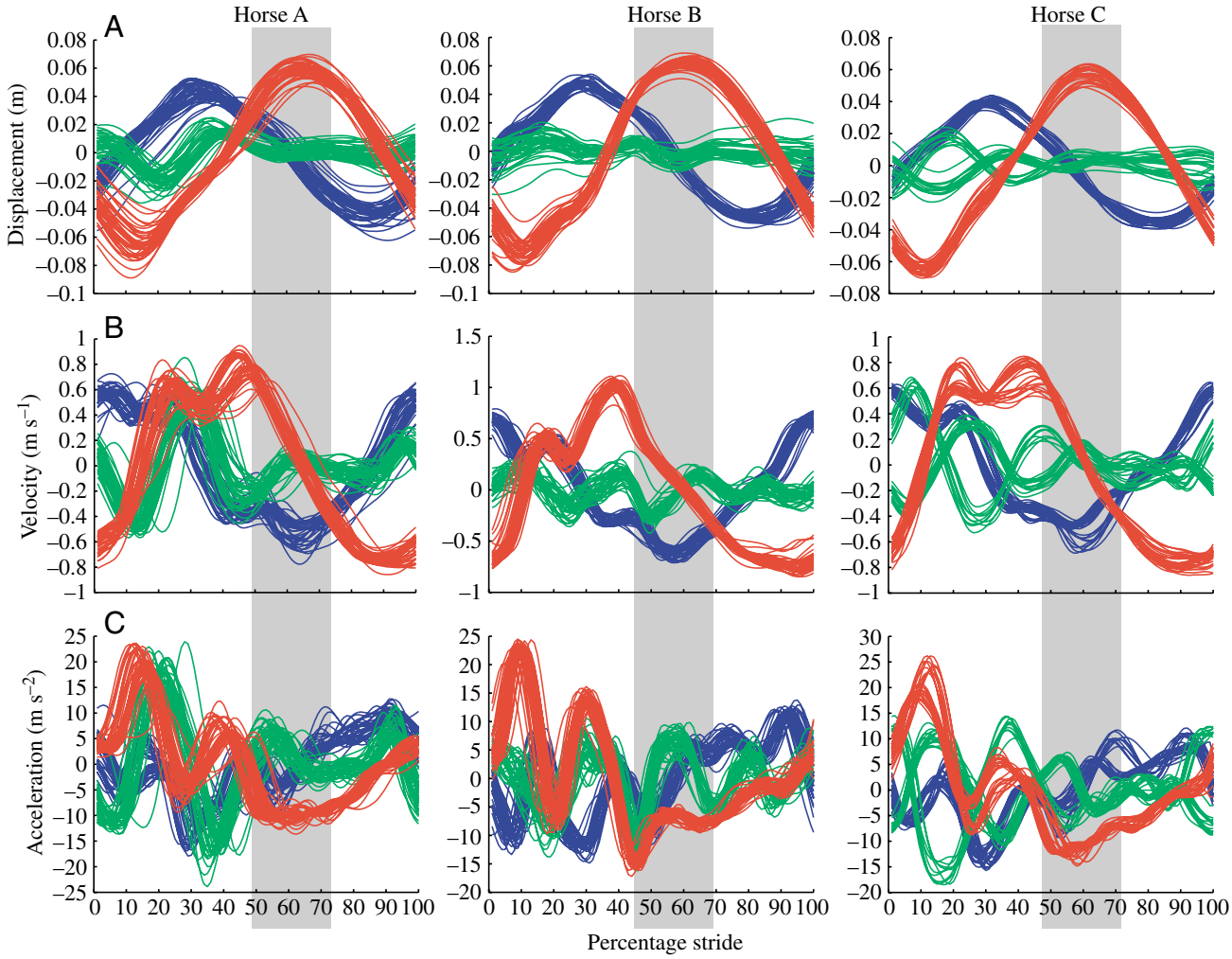

Fig. 4. Individual stride data of three typical horses for craniocaudal (*x*, blue), mediolateral (*y*, green) and dorsoventral (*z*, red) displacement (A), velocity (B) and acceleration (C) of the estimated CoM. Data presented are individual strides between 11.5 m s^{-1} and 12.5 m s^{-1} at gallop. The grey shaded area indicates the measured aerial time with the alignment being based on the assumption that vertical kinetic and potential energy is constant during the aerial phase (see Materials and methods; Fig. 1).

For some horses considerable roll displacement, velocity and acceleration can be observed during the estimated aerial phase (see Discussion for explanation).

Over the speed range analysed here, displacement amplitudes (ranges) generally increased with speed, with the exception of dorsoventral displacement amplitude, which decreased with increasing speed (Fig. 8). Displacement in the craniocaudal direction increased from 75 mm (range 62–88 mm) at 7 m s^{-1} to 89 mm (range 82–97 mm) at 17 m s^{-1} (P<0.05), levelling towards higher speeds. Dorsoventral displacement decreased substantially from 185 mm (range 170–200 mm) at 7 m s^{-1} to 83 mm (range 75–91 mm) at 17 m s^{-1}. Maximum and minimum velocities and accelerations in craniocaudal direction show a slight increase in absolute value with increasing speed, whereas maximum and minimum absolute value of dorsoventral velocity decreased with speed. Dorsoventral acceleration minimum was independent of speed at about –10 m s^{-2} (1 ***g***) experienced during the aerial phase whereas the maximum acceleration slightly decreased with increasing speed.

The amplitude in trunk pitch and heading increased with speed. Pitch range increased from 11.2° (range 10.0–12.4°) to 19.0° (range 18.3–19.7°) and heading range increased slightly from 4.8° (3.8–5.8°) to 7.5° (range 5.8–9.2°) (Fig. 9). Increase in heading velocity and acceleration with speed was found to be more pronounced than increase in pitch velocity and acceleration.

Changes in mechanical energy through the stride for moderate and high speed gallop (12 m s^{-1} and 15 m s^{-1}) are shown in Fig. 10 and Fig. 11, respectively for three typical horses. Fig. 10A and Fig. 11A show the total external mechanical energy and its components (linear kinetic energies, potential energy). In order to be able to compare these energies in one figure, minimum craniocaudal kinetic energy has been subtracted from craniocaudal kinetic and total external energy for each individual stride. Estimated elastic energy stored in the legs (as described in Materials and methods) has been added to this figure. Fig. 10B and Fig. 11B show a more detailed view of the small-amplitude external energies. These are

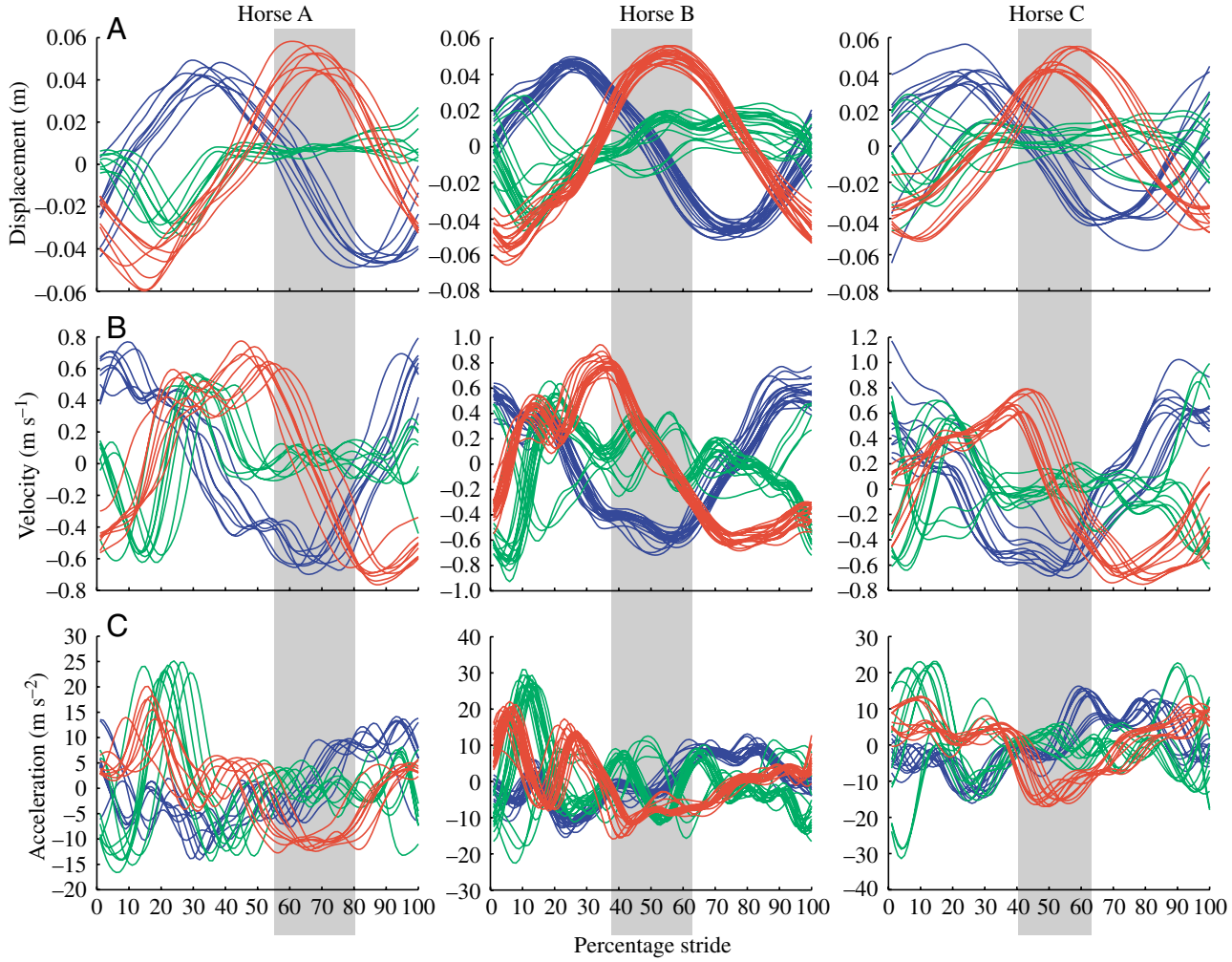

Fig. 5. Individual stride data of three typical horses for craniocaudal (x, blue), mediolateral (y, green) and dorsoventral (z, red) displacement (A), velocity (B) and acceleration (C) of the estimated CoM. Data presented are individual strides between 14.5 m s^{-1} and 15.5 m s^{-1} at gallop. The grey shaded area indicates the measured aerial time with the alignment being based on the assumption that vertical kinetic and potential energy is constant during the aerial phase (see Materials and methods; Fig. 1).

dorsoventral and mediolateral linear kinetic energy and potential energy, and the figures also include components of the internal energy of the trunk: the rotational kinetic energies, which were derived from pitch and heading of the trunk.

Comparison of Fig. 10 and Fig. 11 reveals similar shaped energy curves for the two speeds. External mechanical energy is largely dominated by craniocaudal kinetic energy with a decreasing influence of potential energy with increasing speed (difference between the minima in the plots of total and craniocaudal linear energy), due to increasing amplitude of craniocaudal energy and decreasing amplitude of potential energy. Energy fluctuations during the estimated aerial phase are in general small compared to the time when at least one foot is on the ground (Fig. 10C, Fig. 11C).

Discussion

Gallop is a four-beat gait that is employed by many quadrupeds when travelling at high speed. The mechanics of this asymmetrical gait have yet to be definitively defined. Recently several mechanistic explanations of galloping have been reported. Minetti has described galloping as similar to the bipedal skip, with both gaits employing a combination of pendulum and elastic mechanism (Minetti, 2000). It has also been proposed that galloping may primarily involve the deflection of velocity during the stance phases whilst minimising the variation in speed (Butcher et al., 2001; Ruina et al., 2005). However, no extensive studies of the mechanics of galloping horses travelling over ground at truly high speeds have been performed. This study set out to quantify CoM movement in the horse and to estimate the mechanical energy that this movement entails.

The inertial sensor technique represents the only known method by which trunk movement can be quantified for a continuous series of strides (comprising footfalls of all four feet) during genuine high-speed exercise. Other kinetic and kinematic data collection techniques restrict data collection in practice to the laboratory environment. True high-speed data of horses is not easily available in that environment. Outside the laboratory these techniques are realistically restricted to the

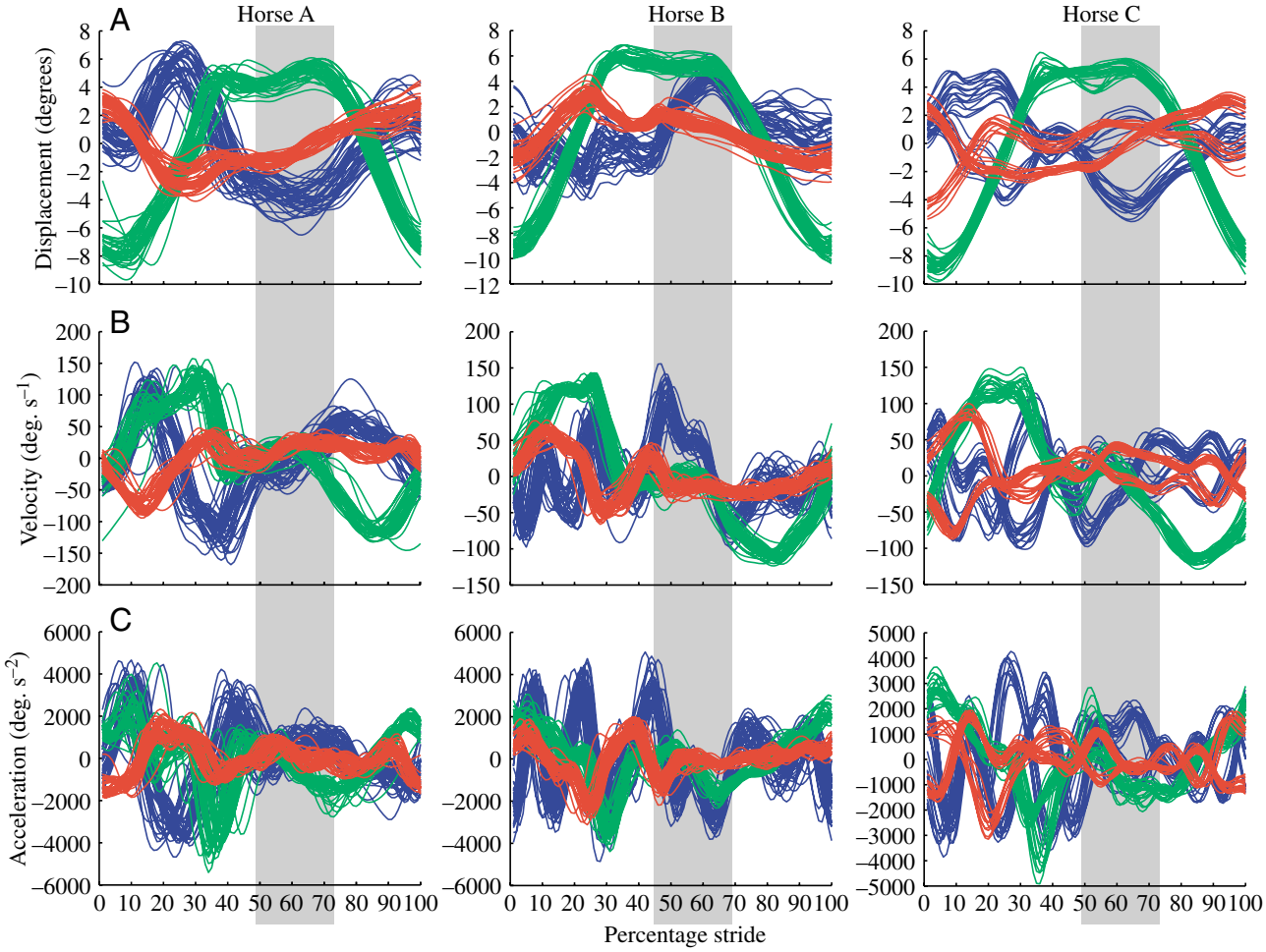

Fig. 6. Individual stride data of three typical horses for roll (blue), pitch (green) and heading (red) displacement (A), velocity (B) and acceleration (C) of the estimated CoM. Data presented are individual strides between 11.5 m s^{-1} and 12.5 m s^{-1} at gallop. The grey shaded area indicates the measured aerial time with the alignment being based on the assumption that vertical kinetic and potential energy is constant during the aerial phase (see Materials and methods; Fig. 1).

collection of data from a few strides (3D motion analysis) or individual stance phases (force plates). Arrays of force plates and 3D motion analysis systems with a sufficient number of cameras are several orders of magnitude more expensive than the mobile data acquisition equipment used in this study and infrared-based 3D optical motion analysis systems are prone to difficulties in daylight. Although inertial sensors have been shown to be accurate for the determination of the movement of a landmark on a subject during cyclical motion (Pfau et al., 2005), their application for the measurement of CoM displacement has yet to be validated. Essential to this method is the projection from the sensor position to the assumed fixed position of the CoM. Here, the sensor is fixed over an external landmark (the withers) and the movement of the sensor is described with 6 d.f. (3 linear and 3 angular displacements). Then the movement of a fixed-point estimate of the CoM 250 mm below and 200 mm behind the sensor position (in the standing horse) is calculated. This is theoretically sufficient to calculate the position of the CoM if the CoM is assumed not to change its position within the body and thus relative to the position of the sensor. The sensitivity analysis applied here to estimate the influence of the assumed position of the CoM on the estimate of mechanical energy was based on one important assumption: the CoM does not move within the animal. In favour of this assumption it can be stated that horses have a relatively low limb mass (5.5% and 5.8% of the whole body mass for the front and hind limbs, respectively) and that it has been observed that a good estimate of CoM displacement can be gained from the measurement of overall trunk movement from a fixed landmark (Buchner et al., 2000). The sensitivity analysis of the relative position of the CoM showed a minimum in external work at a position of 250 mm below and 200 mm behind the sensor, which is close to the position reported previously (Buchner et al., 2000), thus this estimate was used in the data analysis presented here. Adding in internal mechanical energy (angular kinetic energy of the trunk) had little influence on the location of minimum energy fluctuation. Interestingly, the sensitivity analysis showed a bigger change in external mechanical work when deviating from the assumed position in the dorsoventral direction compared to a deviation

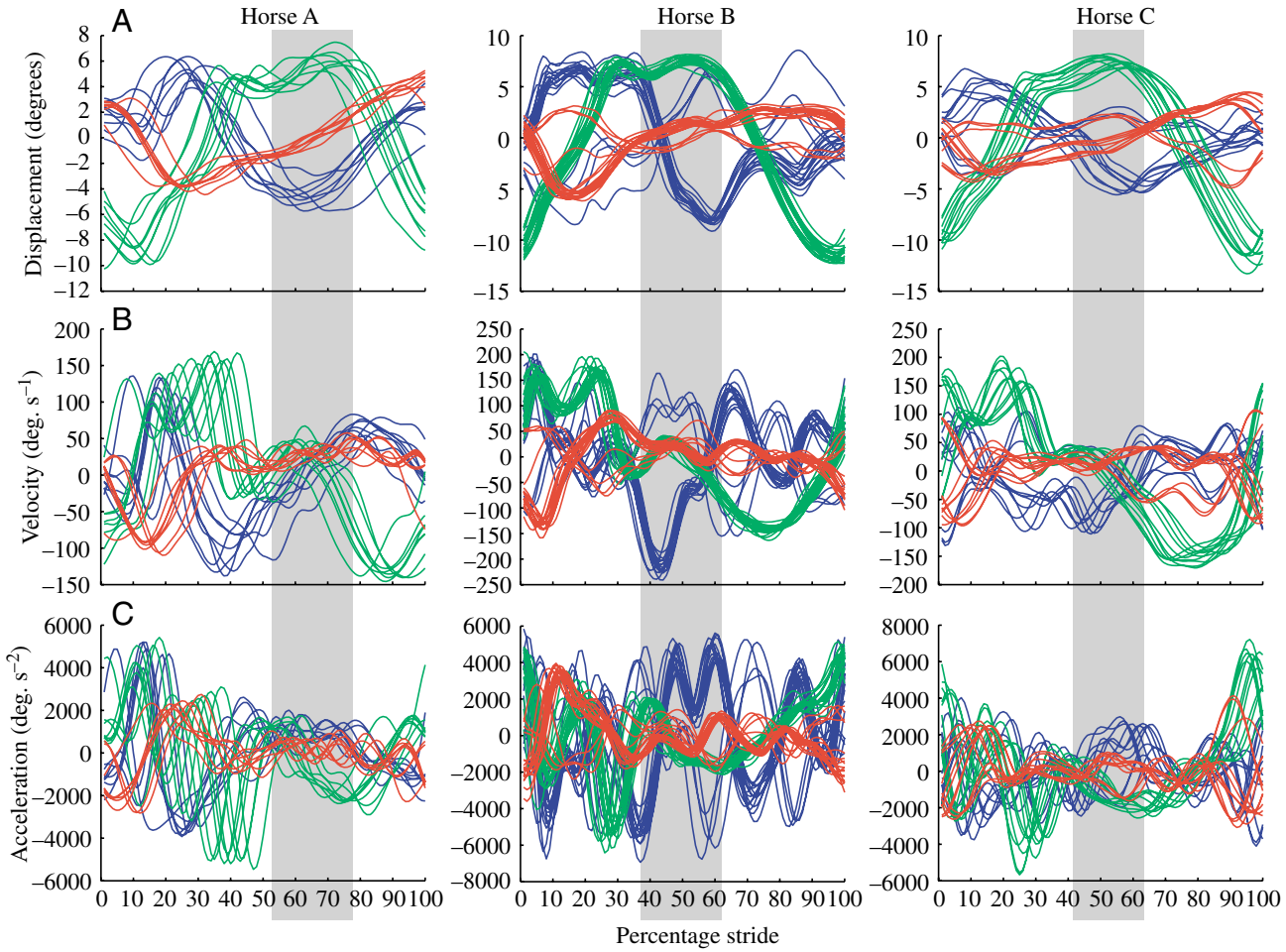

Fig. 7. Individual stride data of three typical horses for roll (blue), pitch (green) and heading (red) displacement (A), velocity (B) and acceleration (C) of the estimated CoM. Data presented are individual strides between 14.5 m s^{-1} and 15.5 m s^{-1} at gallop. The grey shaded area indicates the measured aerial time with the alignment being based on the assumption that vertical kinetic and potential energy is constant during the aerial phase (see Materials and methods; Fig. 1).

in the craniocaudal direction. This might indicate that the method may just be less sensitive to the craniocaudal position of the CoM and maybe that the position of the CoM within the body undergoes bigger changes in the craniocaudal direction during a stride, thus wrong estimates over a whole stride lead to under- or overestimations, which in effect cancel out. Again, this is in agreement with previously reported data (Buchner et al., 2000), which show a smaller R^2 value of 0.37 for the equation relating external trunk landmarks to the craniocaudal movement of the CoM than for the respective equation for dorsoventral movement for which a R^2 of 0.86 is found. Finally, the use of more than one sensor at different locations on the trunk and head may allow motions of the CoM to be determined with greater accuracy.

The measured angular energies were small and dominated by pitch movements (Figs 10, 11). This was significant in magnitude (peaks ~1000 J at 15 m s^{-1}), peaked during the stance phases and was almost zero in the aerial phase. Fluctuation of angular kinetic energy was therefore in phase with the total mechanical energy and does not provide a mechanism for 'storing' energy to reduce total external mechanical energy fluctuations through the stride.

The projection from the sensor position to the assumed position of the CoM implemented here is applied to the displacement data derived from the sensor accelerations and rotations. Inspection of the estimated CoM movement showed relatively large mediolateral movements during the aerial phase, including changes of the direction of movement. We identified this lateral movement and rolling movement of the sensor as a potential source of error (see Figs 6 and 7). One possible explanation for this is that while the forward-backward, up-down, sideways, pitch and heading movement of the sensor was very closely linked to the trunk movement of the horse with the harness being tugged underneath the most cranial edge of the saddle, the harness was strapped to the horse with a surcingle (wide elastic strap around thorax) crossing both shoulders of the horse. Scapula movements (the scapula lies under the attachment and displaces upwards in the stance phase) are likely to introduce a 'pulling' movement (at different times on each side of the horse), which will cause the harness

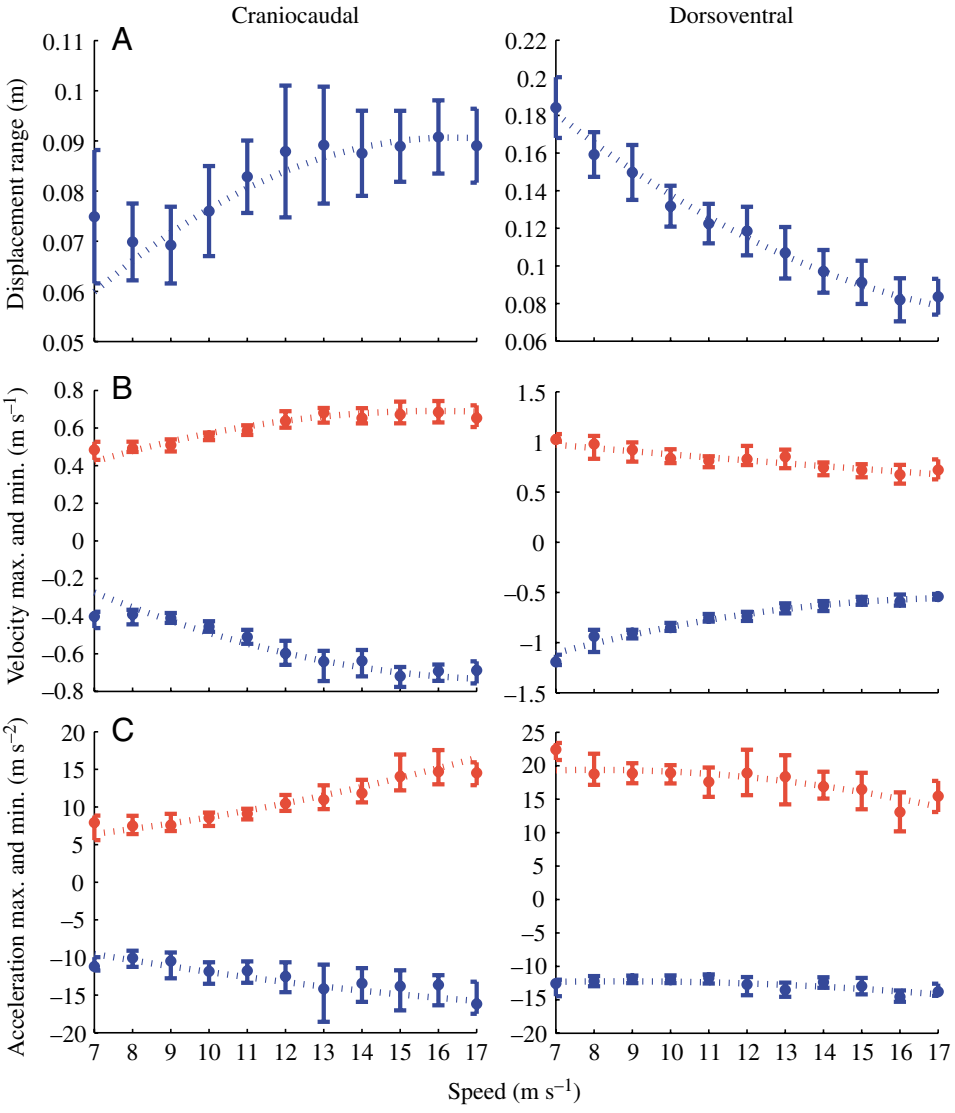

Fig. 8. Displacement range (A) and minimum and maximum velocity (B) and acceleration (C) from 7 m s^{-1} to 17 m s^{-1} for craniocaudal (left) and dorsoventral (right) movement. For each speed category mean and standard deviation (displacement) or median and interquartile range (velocity and acceleration) are given calculated from all strides falling into the respective category. In addition a quadratic function was fitted to the data and is shown as a dotted line.

to tilt around the withers, producing a wrong roll estimate. Assuming all the roll movement to be caused by a rotation of the trunk around the CoM will therefore introduce wrong estimates of mediolateral movement. While roll movement is presented here it was ignored during the calculation of the fixed point estimate of the CoM and roll and mediolateral movement ranges were excluded from the analysis, since maximum and minimum values are likely to be heavily influenced by this effect.

CoM velocities and accelerations then have to be calculated by numerical differentiation of the CoM displacement data. Clearly the differentiation function, which is applied twice (once to the displacement data and once to the velocity data), will influence the shapes of the curves and the values of maximum and minimum values extracted for each stride. Experiments with local regression lines fitted to the data to calculate the local derivative showed that mediolateral velocities and accelerations were more sensitive to the technique used than the corresponding craniocaudal and dorsoventral data.

Mediolateral accelerations seemed large although the displacements were reasonable. This may reflect the above effect, non-cyclical movements distorting the mean subtraction assumption and to a lesser extent also centripetal forces due to the horses going round curved regions of the track. The coordinate system used is aligned with gravity and the long axis of the horse, so even when horses lean into the corner and the force is acting along the legs a centripetal acceleration will occur in the 'mediolateral' direction. Force can only be applied during stance phases and is likely to be greater for some legs than others, so it may create some offset in the data.

The influence of the jockey on the trunk movements observed here was considered to be small. When travelling at high speed, the jockey perches on his toes, with only a very small area of contact to the trunk of the horse. Subjectively, he does not appear to follow the fluctuations in velocity of the horse around the mean progression velocity. Rather, if one were to subtract the progression velocity, the jockey's trunk would be stationary and the horse (and his feet) would move back and forth beneath him. This could cause a small force

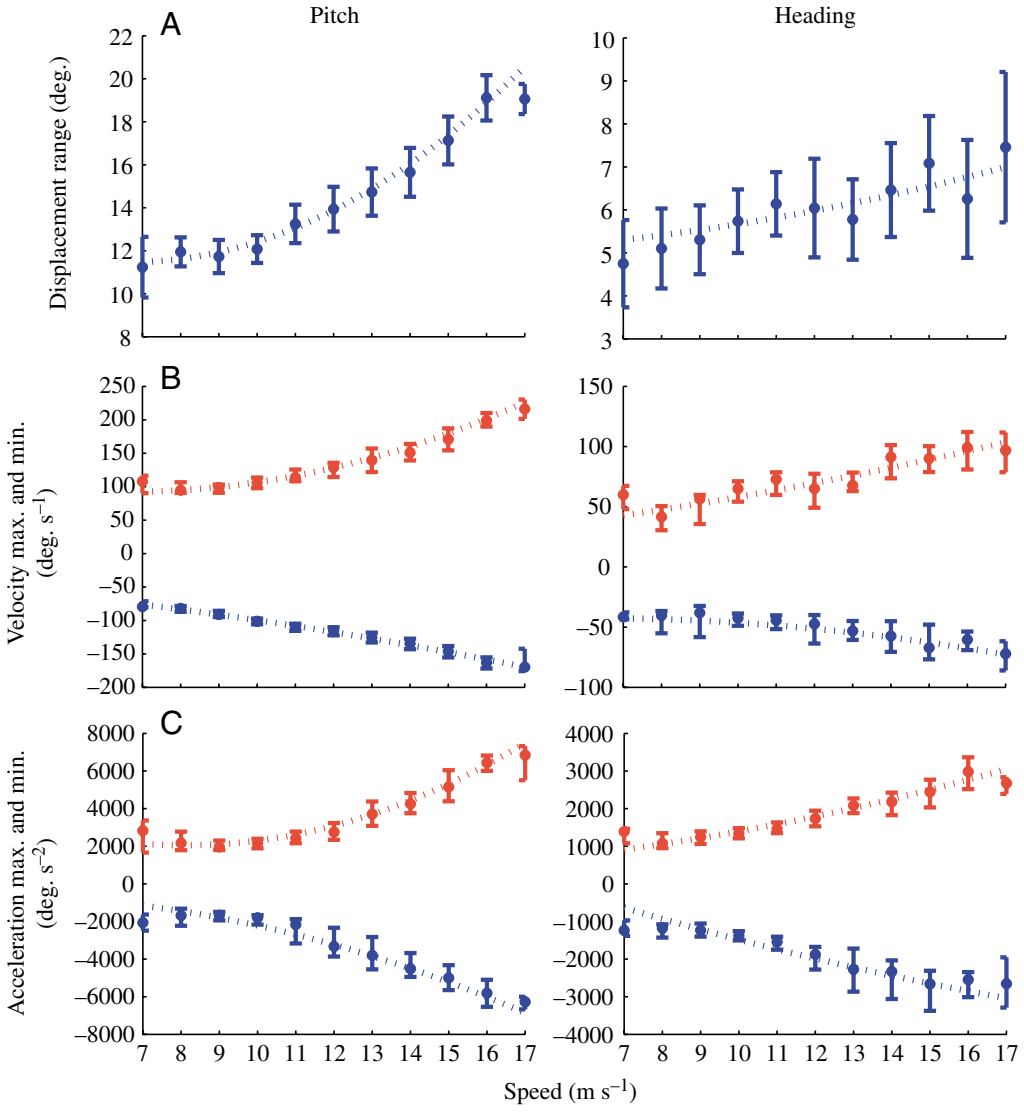

Fig. 9. Displacement range (A) and minimum and maximum velocity (B) and acceleration (C) from 7 m s^{-1} to 17 m s^{-1} for pitch (left) and heading (right) movement. For each speed category mean and standard deviation (displacement) or median and interquartile range (velocity and acceleration) are calculated from all strides falling into the respective category. In addition a quadratic function was fitted to the data and is shown as the dotted line.

acting in the craniocaudal direction, which will effectively appear as an external force in our analysis and thus might explain some of the discrepancies observed during the aerial phase. Interestingly this would imply that the jockey exerts a downward force on the horse and has some vertical inertial influence but would not add to the inertial properties in the horizontal direction. Further studies will be undertaken with an inertial sensor mounted on the jockey as well as the horse and will hopefully clarify this.

In order to assess the validity of the approach presented here, it is interesting to compare the amplitudes of the displacements calculated here with those measured previously during treadmill locomotion at 12 m s^{-1} (Minetti et al., 1999). Vertical displacements concur with those from that study, falling curvilinearly with increasing speed in the 9–17 m s^{-1} speed range. Craniocaudal displacements are however about double those seen by Minetti and co-workers (69 mm *versus* 30 mm at 9 m s^{-1}), and in this study they increase over the range up to 17 m s^{-1}, which was not apparent in the published data. This difference may represent an artefact of the CoM estimation used here or may represent differences in treadmill locomotion. Treadmill belt speed changes (stretching of the belt, slip between drum and belt and deceleration and reacceleration of the moving mass) during the stance phases (Savelberg et al., 1998) might be a confounding factor and moderate the trunk deceleration and acceleration during the stance phase to some extent. Mediolateral displacements were also higher in the data presented here; however, mediolateral forces were variable between individuals and the displacements are comparatively small. Other possible causes are discussed above.

During data analysis, it became evident that the DECT telemetry system introduced a variable delay in the transmission of the inertial sensor data. The exact reasons for this are not clear but are likely to be related to error checking

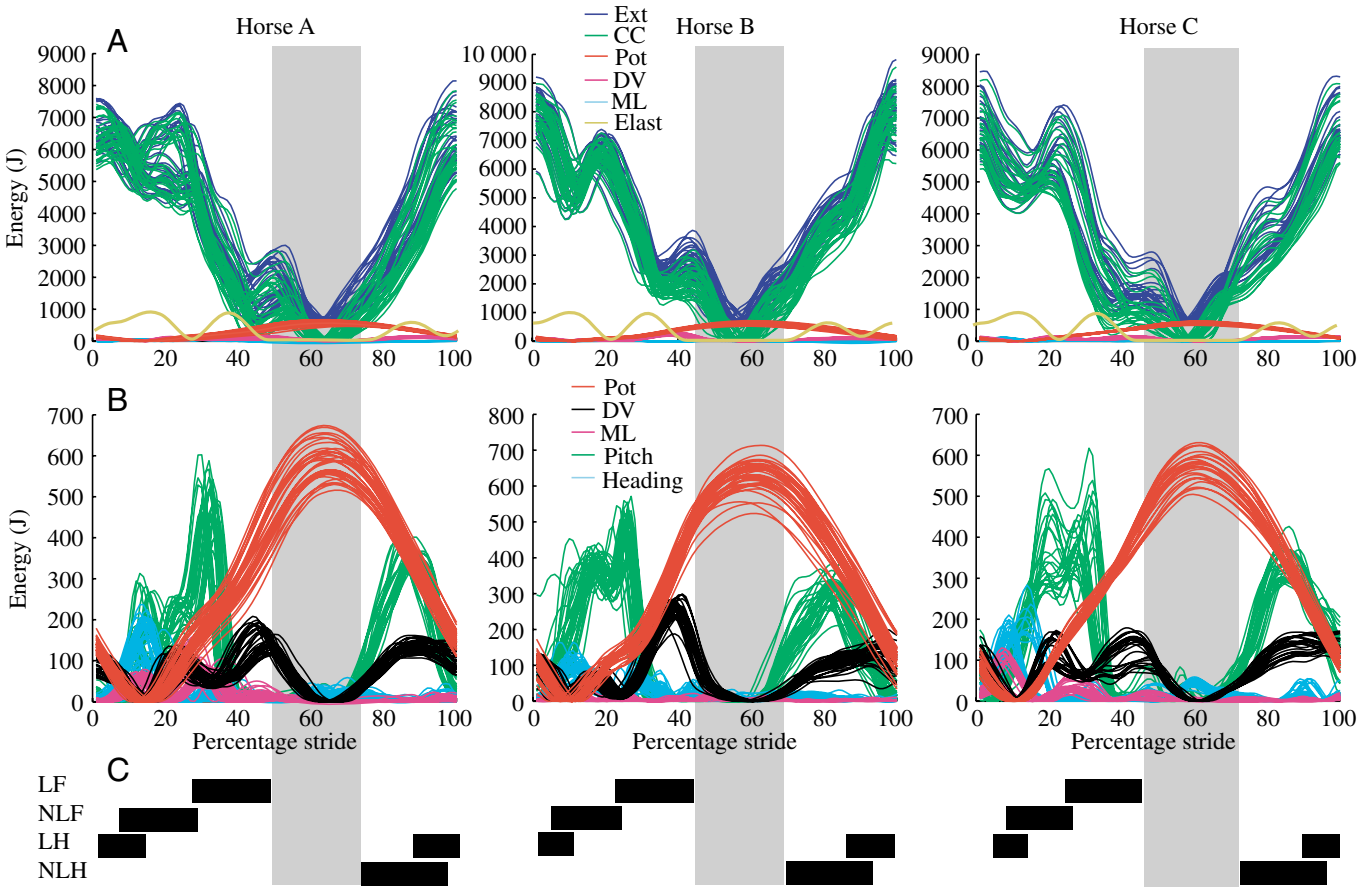

Fig. 10. Individual stride data of changes in external mechanical energy, potential energy and linear kinetic energy (A) and changes in potential, linear and rotational energy (B) as calculated from the movement of the estimated CoM. Data presented are individual strides of three typical horses recorded at speeds between 11.5 m s^{-1} and 12.5 m s^{-1} at gallop. (A) For illustrative purposes the minimum craniocaudal kinetic energy has been subtracted from forward kinetic and external mechanical energy. Ext, external energy (blue); CC, craniocaudal kinetic energy (green); ML, mediolateral kinetic energy (cyan); DV, dorsoventral kinetic energy (magenta); Pot, potential energy (red). Elast, elastic energy estimated from mean footfall pattern at this speed category (light green). (B) Pot, potential energy (red); Pitch, pitch kinetic energy (green); Heading, heading kinetic energy (cyan); ML, mediolateral kinetic energy (magenta); DV, dorsoventral kinetic energy (black). The grey shaded area indicates the measured aerial time with the alignment being based on the assumption that vertical kinetic and potential energy is constant during the aerial phase (see Materials and methods). (C) Stance phases of individual feet are presented as black bars: LF, lead front; NLF, nonlead front; LH, lead hind; NLH, nonlead hind.

methods and serial port buffering. Thus strides were re-segmented using the time of minimum vertical velocity of the trunk sensor as a fixed point within each stride. This was chosen after initial segmentation based upon accelerometer-derived footfall data since minimum vertical velocity approximately corresponds to foot contact of the non-lead front limb (with possible differences between horses and with speed). Therefore, in order to compare the curves produced here to those previously published (Minetti et al., 1999), where the start of the stride was defined as the first foot contact after the aerial phase, the data presented here have to be shifted by approximately 60–80% towards the left. In addition, this delay meant that there was no 'absolute' synchronicity between hoof mounted accelerometers and inertial sensor data, thus aerial times presented in the figures are fitted to the data to our best knowledge. The sum of dorsoventral kinetic and potential energy, as well as dorsoventral acceleration, were the strongest indicators during this procedure. In the absence of any external force (apart from the jockey, see above) during the aerial phase, both of these parameters are theoretically expected to be constant (the latter having a value of –9.81 m s^{-2}). The aerial phases are thus presented in the area where both of these conditions were best met. We were able to confirm the validity of this method in a treadmill experiment where we collected inertial sensor data and high speed video data simultaneously during a medium speed canter.

The patterns of mechanical energy exchange presented here concur with published data (Minetti, 1998; Minetti et al., 1999) showing a bimodal peak in mechanical energy during slow gallop (canter) locomotion. However, Minetti's data show a third peak (approximately coinciding with a peak in potential energy), which is not apparent in our data collected at higher speeds. Unfortunately higher speed data are not presented for the previous study, so differences could also be attributed to a

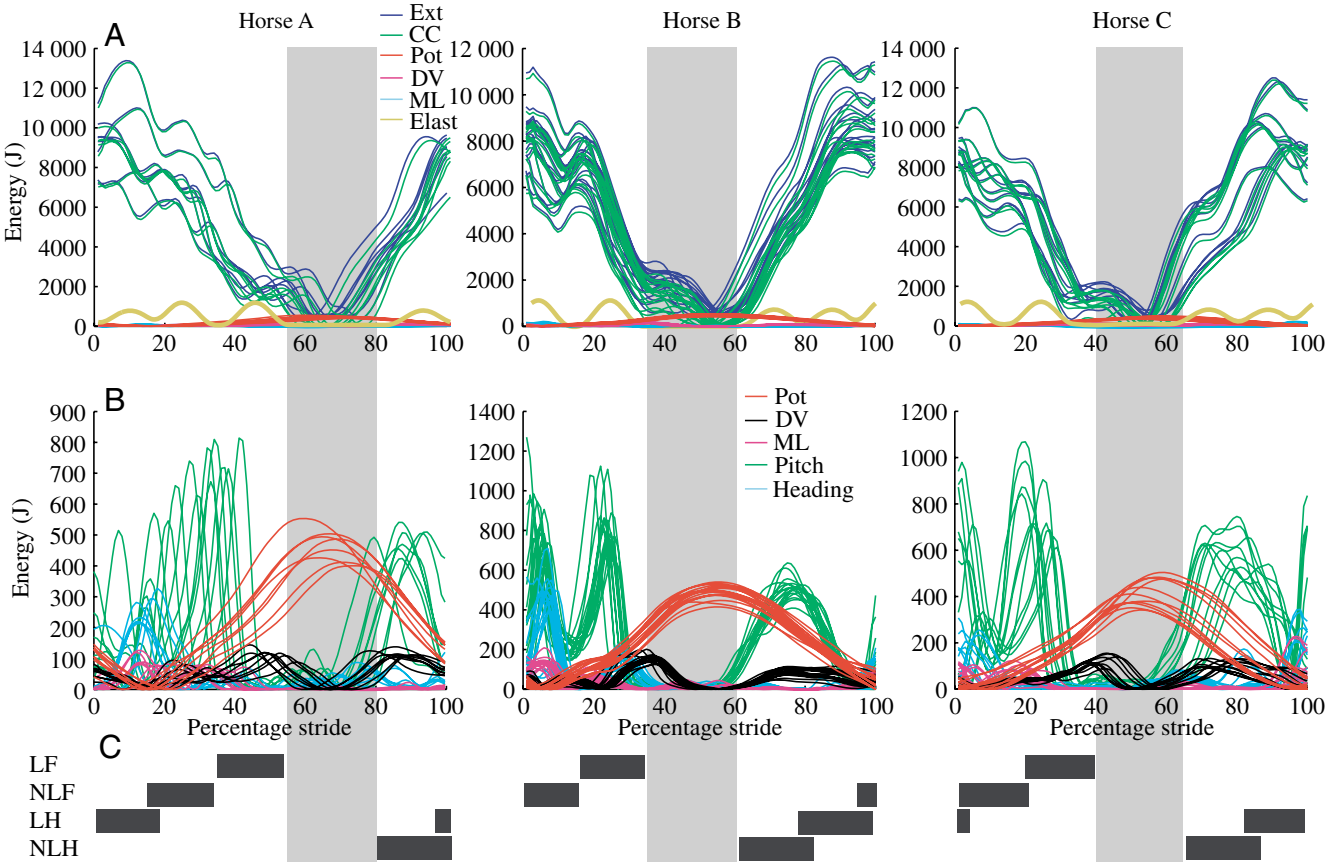

Fig. 11. Individual stride data of changes in external mechanical energy, potential energy and linear kinetic energy (A) and changes in potential, linear and rotational energy (B) as calculated from the movement of the estimated CoM. Data presented are individual strides of three typical horses recorded at speeds between 14.5 m s^{-1} and 15.5 m s^{-1} at gallop. (A) For illustrative purposes the minimum craniocaudal kinetic energy has been subtracted from forward kinetic and external mechanical energy. Ext, external energy (blue); CC, craniocaudal kinetic energy (green); ML, mediolateral kinetic energy (cyan); DV, dorsoventral kinetic energy (magenta); Pot, potential energy (red). Elast, elastic energy estimated from mean footfall pattern at this speed category (light green). (B) Pot, potential energy (red); Pitch, pitch kinetic energy (green); Heading, heading kinetic energy (cyan); ML, mediolateral kinetic energy (magenta); DV, dorsoventral kinetic energy (black). The grey shaded area indicates the measured aerial time with the alignment being based on the assumption that vertical kinetic and potential energy is constant during the aerial phase (see Materials and methods). (C) Stance phases of individual feet are presented as black bars: LF, lead front; NLF, nonlead front; LH, lead hind; NLH, nonlead hind.

gait shift from a slow to medium speed canter (a three-beat gait with a diagonal pair of limbs contacting the ground virtually simultaneously) to a high speed gallop (a true four-beat gait). However, even our lower speed data do not show this feature. Again, treadmill effects could be responsible for some of this difference.

An apparent inconsistency in our external mechanical energy is the fact that craniocaudal and thus total external energy does fluctuate during the aerial phase more and differently than could be expected from wind resistance alone for a passive object. Modelling the aerodynamic drag of a horse by assuming 1 m^2 frontal area with a drag coefficient C_d of 0.7 (e.g. C_d for a human runner, 0.5; C_d for a racing bicyclist, 0.4) leads to a relatively small drag force of 123 N and a power of about 2.1 kW at a speed of 17 m s^{-1} (using the quadratic model for pressure drag). Craniocaudal energy seems to be increasing at the end of the aerial phase before the first hind leg contacts the ground. Likely explanations for this effect include jockey movement (discussed above), movement of the CoM relative to the sensor position, rapid hind leg retraction before foot contact moving the trunk forward (comparable to a child's legs on a swing) as well as errors in sensor orientation and integration inaccuracies (e.g. estimates of initial conditions) from accelerations to velocities at high speed. Also, a change of ±1000 J in craniocaudal energy of a 500 kg horse galloping at an average speed of 15 m s^{-1} corresponds to a change in velocity between 14.86 m s^{-1} and 15.13 m s^{-1}, a relatively small change compared to the overall change of about ±6000 J (14.17 m s^{-1} to 15.78 m s^{-1}). Further studies will aim to use a multi sensor system (head, withers and back of horse as well as jockey) to explore the influence of effects such as relative head and limb movements and movement of the jockey.

Overall, potential energy was greatest during the aerial phase and at a minimum during stance of the two front legs, as would be expected for running gaits. Fluctuation of total mechanical energy was dominated by horizontal kinetic energy (Figs 10, 11). This cycled once per stride with a maximum around the end of hind leg stance and a minimum during the aerial phase. The once per stride cycle is concomitant with the legs functioning in sequence as proposed in Ruina et al.'s model (Ruina et al., 2005). The rise in energy prior to and throughout hind foot contact indicates that the trunk is moving forwards when hind leg retraction occurs (see above) and that work is done throughout hind leg stance by limb retraction. It is known that almost 90% of propulsive musculature is located in the hind legs and mostly as hip extensors (Payne et al., 2004; Payne et al., 2005), thus the hind legs are able to create a substantial torque around the hip. A similar effect can be seen in dogs galloping at relatively low speeds (Cavagna et al., 1977), where little deceleration is found after the aerial phase.

There were fluctuations in total external energy that reflect when energy was stored in the front and hind legs. These fluctuations are, however, smaller than the total change in energy through the stride. This raises the interesting question of whether an additional energy store exists other than the legs or if the fluctuation in mechanical work seen in Fig. 10 is actually dissipated and performed *de novo* in each stride. Some insight can be gained by calculating the mechanical power of galloping (fluctuation of external mechanical energy times stride frequency) from Figs 10 and 11. Fluctuation at 9, 12 and 15 m s^{-1} was 4, 6 and 10 kJ, respectively, through the stride. Multiplying by a stride frequency of 2, 2.1 and 2.25 Hz gives a mechanical power of 8 kW, 12.6 kW and 22.5 kW, respectively. Dividing by speed and body mass gives a mechanical work of transport of 1.6, 1.9 and 2.8 J kg^{-1} m^{-1}, respectively. These values are 55–70% of those presented by Minetti et al., who quote an external mechanical work of 2.3, 3.4 and 4.6 J kg^{-1} m^{-1} for these speeds (Minetti et al., 1999). Those authors, however, observed a metabolic cost of galloping of about 2.5 J kg^{-1} m^{-1}, rising somewhat with speed. Therefore even with our lower figures comparison of the mechanical work performed and the metabolic cost of transport gives an improbably high efficiency of muscle contraction. There must therefore either be an additional energy store acting during the stance phase or we are overestimating mechanical energy fluctuations of the centre of mass.

The spine and hind limb retractors may store some elastic energy during the flight phase (Alexander, 1985) by stretching of the considerable amount of collagenous tissue along the dorsal spine, although spinal flexion has been reported to be relatively small during canter (Faber et al., 2001). It is difficult to estimate how much energy could be stored through this mechanism in the highly pennate spinal extensor muscles present in the horse; however, 7000 J (the total fluctuation in external energy) seems improbably large. Hind limb retraction may increase trunk movement relative to CoM movement, but if this was the source of the discrepancy then Minetti et al.'s data (Minetti et al., 1999) should be more reasonable in terms of efficiency since they calculated the contribution of these segments in their analysis.

Second, gut movements could ameliorate the movement of the CoM that we predict. The abdominal and thoracic contents of a horse comprise about 25% of its body mass. Relative to its mean position the horse goes backward in the aerial phase and during early non-lead hind stance (Figs 4, 5). The onset of inspiration at canter is approximately seen some time between the end of the lead front leg stance phase and the beginning of the aerial phase (Attenburrow, 1982; Lafortuna et al., 1996). This effectively increases the CoM movement in the horizontal direction. Assuming a tidal volume of a galloping horse of about 10–15 l (Lafortuna et al., 1996) and a cross-sectional area of the thorax of about 0.25 m^2, the diaphragm will move by about 0.05 m, which is slightly less than the observed displacement of the trunk. Ventilation should thus increase the actual fluctuation of the horizontal kinetic energy of the CoM relative to trunk movement and not contribute to a reduction of mechanical work. This effect would not be detectable from kinematics but would be apparent in integrated force plate data.

We, like others, are therefore left with the question: how does the horse achieve such improbably high efficiencies? Unfortunately we do not have an explanation but suggest that a combination of spinal energy storage and errors in CoM

determination are likely to account for much of the discrepancy. It would be very interesting to see accurate horizontal force data from a force plate or an instrumented horseshoe for all four legs in a horse undertaking high speed gallop as this would add insight and accuracy to the true fluctuation in horizontal momentum and hence kinetic energy.

The mechanics of gallop have received some attention in recent years (e.g. Minetti, 1998; Minetti et al., 1999; Ruina et al., 2005). It has been likened to a combination of vaulting and running gaits, with Ruina et al.'s model (Ruina et al., 2005) bringing some insight as to why the legs should be used in sequence to create a single 'stance phase'. Our data demonstrate that whilst the legs have spring-like properties, storing and returning mechanical energy during each stance phase (Figs 10, 11), these energies are small in comparison to the total fluctuation in mechanical energy. This difference is a direct effect of high speed over ground locomotion where small fluctuations in horizontal momentum/speed result in large fluctuations in horizontal energy (see above). In terms of mechanical efficiency this indicates that minimising horizontal forces is critical in economical high-speed gait. This must be combined with the demands of providing sufficient vertical impulse to support body weight (and hence maximising duty factor). Spring mass mechanics with the constraints of a fixed protraction time (Robilliard and Wilson, 2006) demonstrate that with increasing speed an increased leg angle is used, which creates a greater horizontal and vertical impulse. Increasing leg stiffness decreases the leg angle used at that speed for the same vertical impulse and hence the horizontal impulse experienced (but at the cost of a shorter contact time and higher peak force). One would assume that maximising stance time carries benefits in constraining peak limb force and achieving economical locomotion (Kram and Taylor, 1991), but it appears here that another pressure may become significant and that horses may sacrifice the benefit of storing all the fluctuation in kinetic energy in the limb. This raises the question of '*what is the optimum limb stiffness*', which is beyond the scope of this study.

The stance timings from these data (Witte et al., 2006) (Witte, 2004) show that the total contact period (i.e. one or more legs on the ground) and the aerial phase duration are almost independent of speed. This is achieved by reducing the fraction of the stride where more than one foot is on the ground and one might imagine that top speed results where this overlap reaches some apparent minimum (Pratt and O'Conner, 1974). There may be one final benefit from overlapping contact phases, which is that one leg can be applying an accelerating force on the CoM whilst another is acting to slow it down, hence cancelling out as occurs in walking (Donelan et al., 2002). Such a locomotor mechanism is explained by the proposed collision model of galloping (Ruina et al., 2005), where legs act in sequence to redirect the CoM. In that model energy is lost during the stance phase. The amount of energy lost is a function of the change in the angle of the trajectory of the CoM (like a bouncing or skimming stone on a hard surface). Examining our data in the light of that model would imply that the lead fore limb is most important in redirecting the CoM since during the stance phase of the lead fore limb the CoM experiences a craniocaudal deceleration, vertical acceleration, and an increase in potential energy. The energy lost is returned throughout the stance phase of both hind legs. This indicates that the work is performed by the powerful hip retractors rather than the leg extensors (Usherwood and Wilson, 2005), otherwise work would be performed during leg extension late in each stance phase.

Conclusions

Mechanical energy fluctuation in the galloping horse is dominated by changes in forward kinetic energy through the stride. Mechanical energy peaks during early fore limb stance and is at a minimum during flight phase. These data are consistent with a collision based model with propulsive effort being provided by retraction of the hind legs.

We would like to thank John Best for providing the horses used in this study, Justine Robilliard for help with data collection, HBLB for funding T.H.W., and BBSRC for funding T.P. A.W. is a BBSRC Research Development Fellow and holder of a Royal Society Wolfson Research Merit award.

References

Ahn, A. M., Furrow, F. and Biewener, A. A. (2004). Walking and running in the red-legged running frog, *Kassina maculate*. *J. Exp. Biol.* **207**, 399-410.

Alexander, R. McN. (1985). Elastic structures in the back and their role in galloping in some mammals. *J. Zool. Lond.* **207**, 467-482.

Alexander, R. M., Maloiy, G. M. O., Hunter, B., Jayes, A. S. and Nturibi, J. (1979). Mechanical stresses during fast locomotion of buffalo (*Syncerus caffer*) and elephant (*Loxodonta africana*). *J. Zool. Lond*. **189**, 135-144.

Attenburrow, D. P. (1982). Time relationship between the respiratory cycle and limb cycle in the horse. *Equine Vet. J.* **14**, 69-72.

Barras, C., Geoffrois, E., Wu, Z. and Liberman, M. (1998). Transcriber: a free tool for segmenting, labeling and transcribing speech. In *Proceedings of the First International Conference on Language Resources and Evaluation (LREC'98)*, pp. 1373-1376, Granada, Spain.

Barrey, E., Galloux, P., Valette, J. P., Auvinet, B. and Wolter, R. (1993). Stride characteristics of overground versus treadmill locomotion in the saddle horse. *Acta Anat. Basel* **146**, 90-94.

Bennett, M. B., Ker, R. F., Dimery, N. J. and Alexander, R. M. (1986). Mechanical properties of various mammalian tendons. *J. Zool. Lond*. **209**, 537-548.

Buchner, H. H., Savelberg, H. H., Schamhardt, H. C., Merkens, H. W. and Barneveld, A. (1994). Kinematics of treadmill versus overground locomotion in horses. *Vet. Q*. **16**, 87-90.

Buchner, H. H., Savelberg, H. H., Schamhardt, H. C. and Barneveld, A. (1997). Inertial properties of Dutch Warmblood horses. *J. Biomech*. **30**, 653-658.

Buchner, H. H., Obermüller, S. and Scheidl, M. (2000). Body centre of mass movement in the sound horse. *Vet. J*. **160**, 225-234.

Butcher, M. T., Bertram, J. E. and Usherwood, J. R. (2001). The geometry of galloping. *Proceedings from the IV World Congress of Biomechanics*.

Cavagna, G. A. (1975). Force platforms as ergometers. *J. Appl. Physiol.* **39**, 174-179.

Cavagna, G. A., Heglund, N. C. and Taylor, C. R. (1977). Mechanical work in terrestrial locomotion: two basic mechanisms for minimizing energy expenditure. *Am. J. Physiol.* **233**, R243-R261.

Donelan, J. M., Kram, R. and Kuo, A. D. (2002). Simultaneous positive and negative external mechanical work in human walking. *J. Biomech*. **35**, 117-124.

Faber, M., Johnston, C., Schamhardt, H. C., van Weeren, P. R.,

Roepsdorf, L. and Barneveld, A. (2001). Three-dimensional kinematics of the equine spine during canter (on a treadmill). *Equine Vet. J. Suppl.* **33**, 145-149.

Ker, R. F. (1981). Dynamic tensile properties of the plantaris tendon of sheep (*Ovis aries*). *J. Exp. Biol*. **93**, 283-302.

Kram, R. and Taylor, C. R. (1990). Energetics of running: a new perspective. *Nature* **346**, 265-267.

Lafortuna, C. L., Reinach, E. and Saibene, F. (1996). The effects of locomotor-respiratory coupling on the pattern of breathing in horses. *J. Physiol*. **492**, 587-596.

McGuigan, M. P. and Wilson, A. M. (2003). The effect of gait and digital flexor muscle activation on limb compliance in the fore limb of the horse (*Equus caballus*). *J. Exp. Biol*. **206**, 1325-1336.

Minetti, A. E. (1998). The biomechanics of skipping gaits: a third locomotion paradigm? *Proc. R. Soc. Lond. B Biol. Sci.* **265**, 1227-1235.

Minetti, A. E. (2000). The three modes of terrestrial locomotion. In *Biomechanics and Biology of Movement* (ed. B. M. Nigg, B. R. MacIntosh and J. Mester), pp. 67-78. Champaign, IL: Human Kinetics.

Minetti, A. E. and Belli, G. (1994). A model for the estimation of visceral mass displacement in periodic movements. *J. Biomech*. **27**, 97-101.

Minetti, A. E., Ardigo, L. P., Reinach, E. and Saibene, F. (1999). The relationship between mechanical work and energy expenditure of locomotion in horses. *J. Exp. Biol.* **202**, 2329-2338.

Ortega, J. D. and Farley, C. T. (2005). Minimizing center of mass vertical movement increases metabolic cost in walking. *J. Appl. Physiol*. **99**, 2099-2107.

Payne, R. C., Veenman, P. and Wilson, A. M. (2004). The role of the extrinsic thoracic limb muscles in equine locomotion. *J. Anat.* **205**, 479-490.

Payne, R. C., Hutchinson, J. R., Robilliard, J. J., Smith, N. C. and Wilson, A. M. (2005). Functional specialisation of pelvic limb anatomy in horses (*Equus caballus*). *J. Anat.* **206**, 557-574.

Pfau, T., Witte, T. H. and Wilson, A. M. (2005). A method for deriving displacement data during cyclical movement using an inertial sensor. *J. Exp. Biol*. **208**, 2503-2514.

Pratt, G. W. Jr and O'Connor, J. T. Jr (1978). A relationship between gait and breakdown in the horse. *Am. J. Vet. Res.* **39**, 249-253.

Riemersma, D. J. and Schamhardt, H. C. (1985). In vitro mechanical properties of equine tendons in relation to cross-sectional area and collagen content. *Res. Vet. Sci.* **39**, 263-270.

Robilliard, J. J. and Wilson, A. M. (2006). Prediction of kinetics and kinematics of running animals using an analytical approximation to the planar spring-mass system. *J. Exp. Biol*. **208**, 4377-4389.

Ruina, A., Bertram, J. E. and Srinivasan, M. (2005). A collisional model of the energetic cost of support work qualitatively explains leg sequencing in walking and galloping, pseudo-elastic leg behavior in running and the walk-to-run transition. *J. Theor. Biol.* **14**, 170-192.

Savelberg, H. H., Vorstenbosch, M. A., Kamman, E. H., van de Weijer, J. G. and Schambardt, H. C. (1998). Intra-stride belt-speed variation affects treadmill locomotion. *Gait Posture* **7**, 26-34.

Usherwood, J. R. and Wilson, A. M. (2005). No force limit on greyhound sprint speed. *Nature* **438**, 753-754.

Witte, T. H. and Wilson, A. M. (2004). Accuracy of non-differential GPS for the determination of speed over ground. *J. Biomech.* **37**, 1891-1898.

Witte, T. H. and Wilson, A. M. (2005). Accuracy of WAAS-enabled GPS for the determination of position and speed over ground. *J. Biomech*. **38**, 1717-1722.

Witte, T. H., Knill, K. and Wilson, A. M. (2004). Determination of peak vertical ground reaction force from duty factor in the horse (*Equus caballus*). *J. Exp. Biol*. **207**, 3639-3648.

Witte, T. H., Hirst, C. V. and Wilson, A. M. (2006). Effect of speed on stride parameters in racehorses at gallop in field conditions. *J. Exp. Biol.* **209**, in press.